Multicritical Point in the Magnetic Phase Diagram of $CsNiCl_3$

M. L. Plumer, Kevin Hood, and A. Caillé
Centre de Recherche en Physique du Solide et Département de Physique, Université de Sherbrooke, Sherbrooke, Québec, Canada J1K 2R1
(Received 6 August 1987)

A phenomenological Landau-type free energy forms the basis of a theory for the low-temperature magnetic properties of $CsNiCl_3$ under the influence of an applied magnetic field. Three magnetically ordered phases, as well as the paramagnetic phase, are found to coexist at a novel type of multicritical point representing the intersection of one line of first-order transitions and three lines of second-order transitions in the H-T phase diagram. The temperature dependences of the critical fields are in good agreement with corresponding experimental data. Similar results are predicted for $CsNiBr_3$.

PACS numbers: 75.30.Kz, 75.40.Cx

There has been considerable interest over the past twenty years in a large class of materials with the generic chemical formula ABX_3 where B is a magnetic ion. Much of this interest has been due to the discovery[1] of quasi one-dimensional magnetic short-range order at low temperatures along the c axis of hexagonal crystals such as $CsNiF_3$ and $CsNiCl_3$. Although it was early recognized that at sufficiently low temperatures most of these materials also exhibit a phase transition to a magnetically ordered state,[2,3] it is only recently that detailed experimental and theoretical work on this aspect of these compounds has been pursued (see Johnson, Rayne, and Friedberg,[4] Matsubara,[5] Rayne, Collins, and White,[6] Miyashita,[7] Kadawaki, Ubukoshi, and Hirakawa,[8] Zhu and Walker,[9] and Plumer and Caillé[10] for some recent examples relevant to the present study). From the results of these studies it is becoming increasingly apparent that this class of materials can have a surprisingly wide range of magnetically ordered phases, many of which are quite novel.

In this Letter, we report on the results of an investigation of the magnetic phase diagram of $CsNiCl_3$ based on a recently developed[10] nonlocal Landau-type free-energy functional. The experimental results of Johnson, Rayne, and Friedberg,[4] who determined the magnetic phase boundaries as functions of temperature and applied magnetic field using susceptibility data, served as an impetus for this work. For the case with $\mathbf{H}$ directed along the hexagonal c axis, they confirmed the previously observed[11,12] spin-flop transition and also found results suggestive of a multicritical point representing the intersection of one line of first-order transitions and three lines of second-order transitions (see Fig. 1). It is a conclusion of the present study that this unusual type of multicritical[13] point is predicted by an analysis of the Landau-type free energy. In addition, we are able to determine the nature of the magnetic ordering which occurs in each phase.

The formulation of a nonlocal Landau free-energy functional of the spin density is presented in Ref. 10 (to be referred to as I) and used there to study the magnetic phase transition in $CsNiF_3$. The interest here, as in I, is in a temperature regime well below the dimensionality crossover temperature where weak interchain exchange coupling produces an effectively three-dimensional magnetic system. Interesting results associated with the higher-temperature quasi one-dimensional magnetic properties of $CsNiCl_3$ have recently been published.[14] Both compounds $CsNiF_3$ and $CsNiCl_3$ belong to the same hexagonal symmetry class $P6_3/mmc$ and have the same form of free energy with differences only in the magnitudes and signs of the expansion coefficients. The spin density is assumed to have the form

$$\mathbf{s}(\mathbf{r}) = (V/N)\sum_{\mathbf{R}} \boldsymbol{\rho}(\mathbf{r})\delta(\mathbf{r}-\mathbf{R}), \tag{1}$$

$$\boldsymbol{\rho}(\mathbf{r}) = \mathbf{m} + \mathbf{S}e^{i\mathbf{Q}\cdot\mathbf{r}} + \mathbf{S}^* e^{-i\mathbf{Q}\cdot\mathbf{r}}, \tag{2}$$

where $\mathbf{R}$ denotes the lattice positions of the Ni^{2+} ions, $\mathbf{m}$

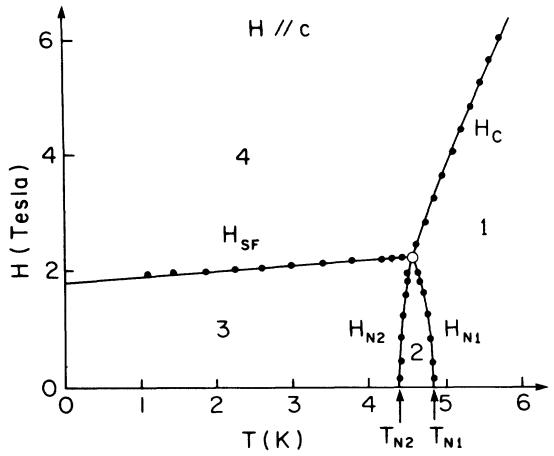

FIG. 1. Magnetic phase diagram for $\mathbf{H} \| \hat{\mathbf{c}}$ showing the boundaries between phases 1–4 as described in the text. Filled circles are from the experimental data of Ref. 4 and the lines represent the fitted theory. Open circle denotes the multicritical point.

is the uniform magnetization induced by the field **H**, and **S** and **Q** are the polarization and wave vectors, respectively, characterizing the long-range magnetic ordering. The free energy appropriate for the study of the magnetic phase transitions in $CsNiCl_3$ is given by

$$F=A_Q S^2-A_z|S_z|^2+B_1S^4+\tfrac{1}{2}B_2|\mathbf{S}\cdot\mathbf{S}|^2+\tfrac{1}{2}\tilde{A}_0m^2-\tfrac{1}{2}A_{z0}m_z^2+\tfrac{1}{4}B_3m^4+2B_4|\mathbf{m}\cdot\mathbf{S}|^2+B_5m^2S^2-\mathbf{m}\cdot\mathbf{H}, \quad (3)$$

where $S^2=\mathbf{S}\cdot\mathbf{S}^*$ and

$$A_Q=a(T-T_Q). \quad (4)$$

The zero-field, low-temperature magnetic structure of $CsNiCl_3$ has been determined by neutron diffraction[3,8] to be characterized by antiferromagnetic ordering along the c axis with an additional period-3 modulation in the basal plane. In I it is shown that (for weak magnetic dipole coupling) the function A_Q is minimized for wave vectors consistent with this structure. The term $-A_z|S_z|^2$ ($A_z>0$) arises from single-ion anisotropy, which is known to be small[14] in this material.

Zhu and Walker[9] have used a free energy similar to (3) to investigate the zero-field magnetic phase transitions in $CsNiCl_3$. The principal features of their results (which are in agreement with neutron-diffraction data[8]) can be summarized as follows. The polarization vector is written as

$$\mathbf{S}=\mathbf{S}_1+i\mathbf{S}_2, \quad (5)$$

where $\mathbf{S}_1$ and $\mathbf{S}_2$ are real vectors given by

$$\mathbf{S}_1=S\cos\beta\hat{\mathbf{z}},\quad \mathbf{S}_2=S\sin\beta\hat{\boldsymbol{\rho}}_2, \quad (6)$$

with $\hat{\mathbf{z}}$ along the c axis and $\hat{\boldsymbol{\rho}}_2$ in the basal plane. Use of (5) and (6) in (3), with $H=m=0$, gives

$$F=A_1S^2+\tfrac{1}{2}BS^4+(A_z-2B_2S^2)S^2\sin^2\beta+2B_2S^4\sin^4\beta, \quad (7)$$

where

$$A_1=a(T-T_{N1}),\quad T_{N1}=T_Q+A_z/a, \quad (8)$$

$B=2B_1+B_2$ and $B_1>0$, $B_2>0$. It is clear that the free energy (7) describes two phase transitions with order parameters S and β. Minimization of (7) results in the following description of the zero-field phases. For $T>T_{N1}$, $S=0$ which we call the paramagnetic phase. In the region $T_{N2}<T<T_{n1}$, $\beta=0$ and $S^2=-A_1/B$ which describes a linearly polarized phase with **S** along the c axis. In the region $T<T_{N2}$, there is a basal-plane component of **S** with $\sin^2\beta=-A_2/(4B_1S^2)$ where

$$A_2=a(T-T_{N2}),\quad T_{N2}=T_{N1}-A_zb/a, \quad (9)$$

and $b=B/(2B_2)$. This describes an elliptically polarized spin structure where **S** is confined to the $z\rho_2$ plane. Zhu and Walker[9] have shown that $\hat{\boldsymbol{\rho}}_2$ can lie along one of the three basal-plane crystallographic axes as a result of sixth-order anisotropy contributions to the free energy in agreement with neutron-diffraction data.[3,8] A variety of experimental results (see Ref. 8 for a review) give $T_{N1}\cong 4.85$ K and $T_{N2}\cong 4.40$ K.

We consider now the effect of applying a magnetic field along the c axis. The terms $-\frac{1}{2}A_{z0}m_z^2$ ($A_{z0}>0$) and $-\mathbf{m}\cdot\mathbf{H}$ in (3) are minimized with **m** parallel to **H**. Any deviation from this configuration is due to the term $B_4|\mathbf{m}\cdot\mathbf{S}|^2$ which is small compared with $|\mathbf{m}\cdot\mathbf{H}|$ (for small S). We thus assume that **m** is also along the c axis. Field-induced changes in the zero-field form of the polarization vector **S**, given by (5) and (6), are also caused by this coupling term which (with $\mathbf{m}\parallel\hat{\mathbf{z}}$) is now given by $B_4m^2|S_z|^2$. It is assumed here that $B_4>0$ so that this term is minimized with $|S_z|=0$. A simple generalization of (6) which allows for the possibility that $|S_z|=0$ with $S_1\neq 0$ is to take

$$\mathbf{S}_1=S\cos\beta[\sin\theta\hat{\boldsymbol{\rho}}_1+\cos\theta\hat{\mathbf{z}}], \quad (10)$$

where θ is to be determined and $\mathbf{S}_2$ retains its zero-field form (6). In this expression, $\hat{\boldsymbol{\rho}}_1$ is chosen to be in the basal plane perpendicular to $\hat{\boldsymbol{\rho}}_2$ as this configuration minimizes the term $\frac{1}{2}B_2|\mathbf{S}\cdot\mathbf{S}|^2$ in (3). The free energy can now be expressed as

$$F=C_sS^2-C_\theta S^2\cos^2\theta+C_\beta S^2\sin^2\beta+2B_2S^4\sin^4\beta+\tfrac{1}{2}A_0m^2+\tfrac{1}{2}BS^4+\tfrac{1}{4}B_3m^4-mH, \quad (11)$$

where $C_s=A_Q+B_5m^2$, $C_\theta=A_z-2B_4m^2$, $C_\beta=C_\theta\cos^2\theta-2B_2S^2$, and $A_0=\tilde{A}_0-A_{z0}\equiv a(T-T_0)$. In addition to the zero-field order parameters S and β, the angle θ also characterizes a phase transformation; it undergoes a first-order change from its low-field value $\theta=0$ to a high-field value $\theta=\pi/2$, which describes a spin-flop transition. It is also clear from (11) that the coefficients C_s, C_θ, and C_β all vanish at a single multicritical point in the phase diagram. This point (T_m,H_m) can be determined by our solving the equations $C_s=0$, $C_\theta=0$ along with $S=0$ and $\partial F/\partial m=0$ to obtain

$$T_m=T_{N1}-A_zB_6/(2aB_4), \quad (12)$$

$$H_m=(A_z/2B_4)^{1/2}[\Delta+(A_z/2B_4)(B_3-B_5)], \quad (13)$$

where $B_6=2B_4+B_5$ and where $\Delta=A_0-A_Q$ is independent of temperature. From Fig. 4 of Ref. 4 the estimates $T_m\cong 4.6$ K and $H_m\cong 2.29$ T can be made.

Minimization of the free energy (11) with respect to S, β, and θ reveals that there are four magnetic phases characterized as follows:

(1) paramagnetic: $S=0$; (2) linear: $\beta=0$, $\theta=0$; (3) elliptical: $\sin^2\beta=-C_\beta/(4B_2S^2)$, $\theta=0$; (4) 120° structure: $\beta=\pi/4$, $\theta=\pi/2$. The so-called 120° structure is simply a helically polarized phase with an associated wave vector in the plane of $\mathbf{S}_1$ and $\mathbf{S}_2$ (the basal plane), as discussed in I.

The temperature dependences of the critical fields which determine the phase boundaries associated with the second-order transitions 1–4, 1–2, and 2–3 can be obtained by an analysis of the free energy and are given by (see Fig. 1)

$$H_c=(-A_Q/B_5)^{1/2}[\Delta+(1-B_3/B_5)A_Q], \tag{14}$$

$$H_{N1}=(-A_1/B_6)^{1/2}[A_0+(B_3/B_6)A_1], \tag{15}$$

$$H_{N2}=\left(\frac{A_2}{B_7}\right)^{1/2}\left[A_0-2\left(\frac{B_6}{B_1}\right)A_1+\left(\frac{B_8}{B_7}\right)A_2\right], \tag{16}$$

where $B_7=BB_4/B_2-B_6$ and $B_8=B_3-2B_6^2/B$. The spin-flop phase boundary $H_{sf}(T)$ must be determined numerically by a comparison of the free energies for phases 3 and 4. This has been done (and the above analytical results have been verified) with use of estimates for the phenomenological coefficients which appear in (11) by a comparison of the above theory with the experimental data of Ref. 4, as described below.

For these numerical estimates, cgs units (with the magnetization expressed in electromagnetic units per gram) are used. From the expression $m^2=\frac{1}{2}A_z/B_4$ (valid at the multicritical point) and the magnetization data, the estimate $\frac{1}{2}A_zB_4\cong 1.92$ can be made. Extrapolation of the data for $H_c(T)$ to zero field gives $T_Q\cong 4.3$ K. Comparison of the expressions for H_m and $H_c(5.5\text{ K})$ with the data then yields $\Delta\cong 1.56\times 10^4$ and $B_3-B_5\cong 460$. The data and expressions for T_m-T_{N1}, $T_{N1}-T_Q$, and $T_{N1}-T_{N2}$ then give $A_z/a\cong 0.55$, $b=B_1/B_2+\frac{1}{2}\cong 0.82$, $B_4/a\cong 0.14$, and $B_5/a\cong -0.16$. All of the parameters of the theory except B_1 (or equivalently B_2) and a can thus be determined by m^2 at (T_m,H_m), $H_c(T)$ and the three points in the phase diagram T_{N1}, T_{N2}, and (T_m,H_m). It is then possible for us to fit $H_{sf}(T)$, as determined numerically, to the data by choosing any reasonable value for B_1/a and subsequently adjusting the value of a. The choice $B_1/a=0.1$ gives $a\cong 400$ and the theoretical curves shown in Fig. 1 result. Because of the large number of adjustable parameters, the resulting excellent agreement between theory and experimental data may only indicate that the model presented here gives a correct qualitative understanding of the magnetic phase diagram.

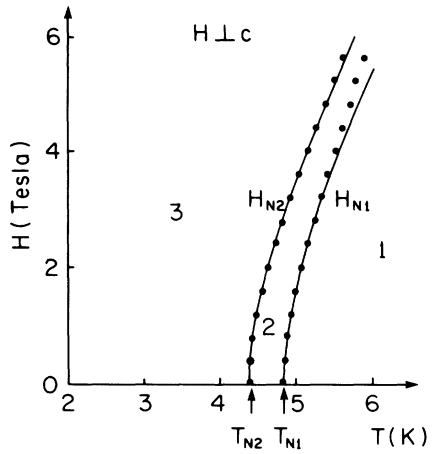

FIG. 2. Phase diagram for $\mathbf{H}\perp\hat{\mathbf{c}}$ showing results of the theory (lines) and experimental data (circles) of Ref. 4.

As a further check that the above model for the magnetic phases of $CsNiCl_3$ is correct, the phase diagram for the case with $\mathbf{H}$ applied in the hexagonal basal plane can be determined and compared with corresponding data from Ref. 4. It is assumed here that $\mathbf{m}$ is parallel to $\mathbf{H}$ and perpendicular to $\hat{\boldsymbol{\rho}}_2$ and that the zero-field structure of the polarization vector $\mathbf{S}$ given by (5) and (6) remains valid. These assumptions are consistent with the previously made arguments for the case of $\mathbf{H}\parallel\hat{\mathbf{z}}$. The magnetic phase diagram then consists of the three phases 1, 2, and 3 with phase boundaries (see Fig. 2) given by

$$H_{N1}=(-A_1/B_5)^{1/2}[\tilde{\Delta}+A_z+(1-B_3/B_5)A_1], \tag{17}$$

$$H_{N2}=(-A_2/B_5)^{1/2}[\tilde{\Delta}+A_Q+(B_5/B_2)A_z-(B_3/B_5)A_2], \tag{18}$$

where $\tilde{\Delta}=\Delta+A_{z0}$. All of the parameters appearing in these expressions have been previously determined except for A_{z0}. The choice $A_{z0}\cong 400$ results in the good agreement with the measured data as shown in Fig. 2.

Some of the gross features of the $\mathbf{H}$-T diagram can be understood with simple arguments. The suppression or enhancement of the critical temperatures with a magnetic field is a consequence of $\mathbf{H}$ (and $\mathbf{m}$) being respectively parallel or perpendicular to the spin $\mathbf{S}$ of the lower-temperature ordered phase. This view is consistent with the negative slope of H_{N1} with $\mathbf{H}\parallel\hat{\mathbf{c}}$ and the positive slopes of the other second-order transition lines in Figs. 1 and 2. These features can be traced to the result that B_4 is positive and B_5 is negative in the free energy (3).

We can tentatively attribute to the different phases in Fig. 1 the following effective spin dimensionalities n_s: $n_s=1$ in the linear phase and $n_s=2$ for both the elliptical and 120° structures. As a result, the effective spin dimensionality at

the multicritical point should be $n_s = 3$. Since this multicritical point also represents a novel convergence of three second-order phase-transition lines with the first-order spin-flop line, interesting critical behavior may occur in this region of the phase diagram; in particular, behavior associated with effective spin dimensionality crossover.

$CsNiBr_3$ exhibits two magnetic phase transitions in the absence of a magnetic field at $T_{N1} \cong 14.3$ K and $T_{N2} \cong 11.8$ K where a variety of experimental data[15] suggest that the magnetic orderings involved are the same as in $CsNiCl_3$. A similar magnetic phase diagram can thus be expected for this material and measurements of its magnetic properties in an applied magnetic field are desirable.

In summary, it has been demonstrated here by an analysis of a recently developed[10] nonlocal Landau free-energy functional, in conjunction with the experimental results of Ref. 4, that a novel type of multicritical point exists in the magnetic phase diagram of $CsNiCl_3$. Further experimental work (e.g., neutron diffraction), to verify the predicted spin structures, and theoretical study of the associated critical behavior are desirable.

We thank X. Zhu and M. Walker for sending us a preprint of their paper. This work was supported by the National Sciences and Engineering Research Council of Canada and by Fonds FCAR pour l'Aide et le Soutien à la Recherche du Gouvernement du Québec.

[1]N. Achiwa, J. Phys. Soc. Jpn. **27**, 561 (1969); M. Steiner, J. Villain, and C. G. Windsor, Adv. Phys. **25**, 87 (1976).

[2]M. Steiner, Solid State Commun. **11**, 73 (1972).

[3]W. B. Yelon and D. E. Cox, Phys. Rev. B **7**, 2024 (1973).

[4]P. B. Johnson, J. A. Rayne, and S. A. Friedberg, J. Appl. Phys. **50**, 1853 (1979).

[5]F. Matsubara, J. Phys. Soc. Jpn. **51**, 2424 (1982).

[6]J. A. Rayne, J. G. Collins, and G. K. White, J. Appl. Phys. **55**, 2404 (1984).

[7]S. Miyashita, J. Phys. Soc. Jpn. **55**, 227 (1986), and **55**, 3605 (1986).

[8]H. Kadawaki, K. Ubukoshi, and K. Hirakawa, J. Phys. Soc. Jpn. **56**, 751 (1987).

[9]X. Zhu and M. B. Walker, Phys. Rev. B **36**, 3830 (1987).

[10]M. L. Plumer and A. Caillé, to be published.

[11]D. P. Almond and J. A. Rayne, Phys. Lett. **55A**, 137 (1975).

[12]E. Cohen and M. D. Sturge, Solid State Commun. **24**, 51 (1977).

[13]For reviews on multicritical phenomena, see, e.g., *Critical Phenomena,* edited by F. J. W. Hahne, Lecture Notes in Physics Vol. 186 (Springer-Verlag, Berlin, 1983); *Multicritical Phenomena,* edited by R. Pynn and A. Skjeltorp, NATO Advanced Study Institute Series B, Vol. 106 (Plenum, New York, 1983); Y. Shapira, J. Appl. Phys. **57**, 3268 (1985).

[14]W. J. L. Buyers, R. M. Morra, R. L. Armstrong, M. J. Hogan, P. Gerlach, and K. Hirakawa, Phys. Rev. Lett. **56**, 371 (1986).

[15]R. Brener, E. Ehrenfreund, H. Shechter, and J. Mavosky, J. Phys. Chem. Solids **38**, 1023 (1977).